SF2A 2010
S. Boissier, M. Heydari-Malayeri, R. Samadi and D. Valls-Gabaud (eds)

DUST IN MOLECULAR CLUMPS FROM THE HI-GAL SURVEY

D.J. Marshall[1], L.A. Montier[1], I. Ristorcelli[1], L. Anderson[2], J.P. Bernard[1] , C. Brunt[3], P. Martin[4], J. Mottram[3], D. Paradis[5] and J. Rodon[2]

Abstract. Dust properties in molecular clouds may give clues to the star formation process. By using recent observations of dust and gas emission, we seek to constrain the dust properties in discrete molecular clumps in the plane of the Milky Way. Using observations of the interstellar gas, we separate observed dust emission from the Hi-GAL survey, using the Herschel Space Observatory, into discrete line of sight components. A new dust spectral inversion technique is used where the dust emission is assumed to be a linear sum of a finite number of components, where the emission from each component follows a modified blackbody emission law. We are able to obtain the dust properties in over 60 molecular clumps in a 4 square degree zone centred on l=30°, b=0°. The dust in a few of the molecular clumps is found to be warmer than the dust associated with the atomic phase of the gas. This suggests that these clumps are not heated solely by the interstellar radiation field, but also contain an internal heating source suggesting the onset of an initial stage of star formation.

Keywords: ISM: clouds, galaxy: disk, infrared: ISM

1 Introduction

Hi-GAL (Molinari et al. 2010a) is a Key-Project of the Herschel Space Observatory that is using 343 hours observing time to carry out a 5 band photometric imaging survey at 70, 160, 250, 350 and 500 μm of a 2 degree wide strip of the Milky Way Galactic Plane in the longitude range $-60^{o} \leq l \leq 60^{o}$. The dust properties inferred from the dust emission provides us with crucial information on the physical state of the ISM. The conditions within molecular clouds are particularly interesting as these are the future sites of star formation. However, the derivation of dust properties within molecular clouds is not trivial as many line of sight components contribute to the dust emission. We present a new method to obtain the dust properties within individual molecular cores.

2 Data

We use Herschel SDP observations at l=30 and b=59 from the Hi-GAL survey (Molinari et al. 2010b), HI data from the VGPS (Stil et al. 2006) and ^{12}CO from the GRS (Jackson et al. 2006) along with a CO clump catalogue (Rathborne et al. 2009). All observations have been degraded to a common angular resolution of 1'.

3 Three dimensional inversion

3.1 Classic inversion methods

The dust emission associated with a molecular core can be difficult to identify in the Hi-GAL data. We use a catalogue of CO cores and proceed with an inversion technique to extract the dust properties of the cores.

Classical inversion methods (Giard et al. 1994; Sodroski et al. 1997; Paladini et al. 2007) seek to invert the full sky dust emission into a number of Galactocentric radii in order to study dust properties as a function of Galactic position and

[1] Universit de Toulouse, UPS, CESR, CNRS, UMR5187, 9 avenue du colonel Roche, F-31028 Toulouse cedex 4, France
[2] Laboratoire d'Astrophysique de Marseille (UMR 6110 CNRS & Universit de Provence), 38 rue F. Joliot-Curie, 13388 Marseille, Cedex 13, France
[3] University of Exeter, Physics Building, Stocker Road, Exeter EX4 4QL, UK
[4] Canadian Institute for Theoretical Astrophysics, University of Toronto, 60 St. George Street, Toronto, ON M5S 3H8, Canada
[5] Spitzer Science Center, California Institute of Technology, CALTECH, 1200 East California Boulevard, MC 220-6, Pasadena, CA 91125, USA

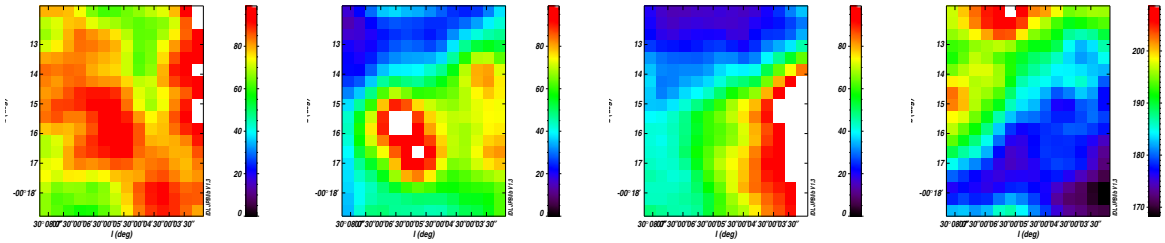

Fig. 1. Components used in the inversion for the CO core G029.89-00.26_c4. From left to right are: CO_{before}, CO_{clump}, CO_{after} and HI. Before and after refer to the radial velocity with respect to the clump and are not necessarily physically before and after the CO clump.

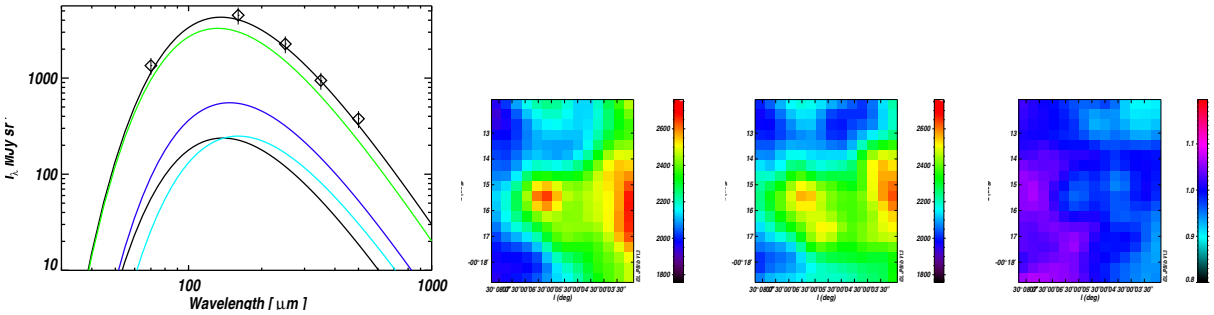

Fig. 2. Left: SEDs for the components presented in Fig.1 : HI(green), CO_{before}(black), CO_{clump}(dark blue) and CO_{before}(light blue). The total of all components (solid line) is compared to the average observed spectrum by Herschel (diamonds). **Right**: Original Hi-GAL 250 μm image, modelled observations and ratio of model/observations. It can be seen that the model accounts very well for the dust emission throughout the selected region.

in each phase of the interstellar gas (atomic, molecular and ionised). The radial velocity of the gas is used to separate the Galactic gas emission into a number of Galactocentric rings and then the dust emissivity for each ring in each gas phase is calculated. The problem being solved can be written, for any dust observation I_λ, as:

$$I_\lambda = \Sigma_{i=1}^{n} \left(\epsilon_{H_I}(R_i, \lambda) N^i_{H_I} + \epsilon_{H_2}(R_i, \lambda) N^i_{H_2} + \epsilon_{H_{II}}(R_i, \lambda) N^i_{H_{II}} \right) \tag{3.1}$$

where the sum is over a number (n) of Galactocentric rings (denoted by the index i) and where N_{H_I}, N_{H_2} and $N_{H_{II}}$ are the total gas column density of the gas observations in each ring i for the atomic, molecular and ionised components, respectively. The result of this inversion is the dust emissivity ϵ per ring and per phase of the gas.

3.2 Dust spectral inversion

For the problem at hand, namely to isolate the dust properties within individual molecular clumps, classic inversion methods are not adequate. Indeed there are a number of free parameters which require a large number of pixels in order to have more equations than unknowns. Using higher resolution data which is now becoming available in the plane of the Galaxy does help a great deal in reducing the minimum size of the regions which can be inverted. However when the inversion is applied band by band to small zones it is not uncommon for the inversion technique to provide mathematically good solutions which are not physical. A simple example would be negative emissivities which provide a good solution to Eq.3.1 but which obviously provides an unsatisfactory solution.

As such, we have proceeded with a slight twist on the classic inversion methods by assuming, apriori, that the spectral energy distribution (SED) of the different components are all dominated by dust in thermal equilibrium. We model such dust by a modified blackbody, where at a frequency ν and for a dust temperature T, the observed flux I_ν is given by:

$$I_\nu = B(\nu, T)\nu^{-\beta} \tag{3.2}$$

where β is the spectral index.

The inversion equation thus becomes:

$$I_{\nu_1..\nu_n} = \Sigma_{i=1}^{n} \epsilon_{H_I}(i) B(\nu_1..\nu_n, T_i)\nu^{-\beta_i} + \epsilon_{H_2}(i) B(\nu_1..\nu_n, T_i)\nu^{-\beta_i} \tag{3.3}$$

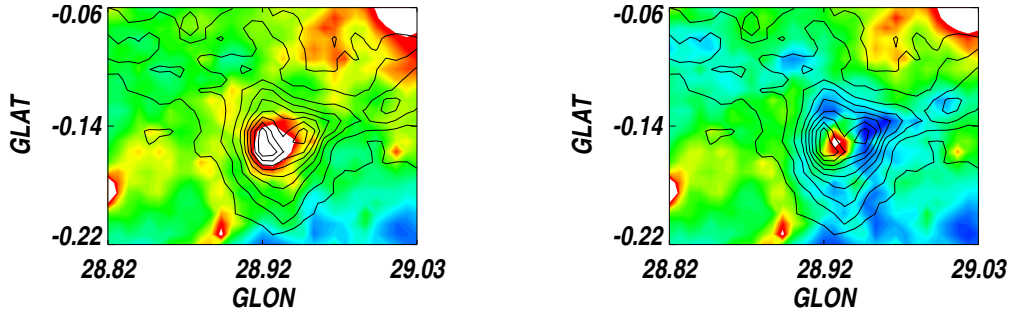

Fig. 3. Residue in the fitting procedure for clump G029.14-00.16_c3. **LEFT**: Original Hi-GAL 250 μm image with CO clump contours. **RIGHT**: Observed Hi-GAL image with CO clump contribution removed. Note that only the dust emission associated to the clump has been removed and not the dust associated with all CO.

thus there are three parameters per component and all frequencies are adjusted simultaneously. This reduces the degrees of freedom of the problem and ensures that the spectra obtained for the components is indeed a modified blackbody.

As an example, a set of components is shown in Fig.1. The second component from the left is the CO emission integrated over the FWHM velocity range of the CO clump from Rathborne et al. (2009). The component on either side of the clump are the CO emission integrated up to the clump and after the clump, respectively. The fourth component is the total line of sight HI gas.

The appropriate ϵ and T are solved for each component via the above inversion method, while keeping $\beta = 2$. The resulting SEDs from this inversion are shown on the left side of Fig.2, and where the total SED is compared to the observed average SED. It should be stressed that the SEDs for each pixel are being solved for simultaneously. Using the derived parameters it is possible to reconstruct the observed image using the gaseous templates. This is shown on the right side of Fig.2. The modelled dust emission (middle) is obtained by using each of the gaseous components and applying the appropriate derived ϵ, T pair and then summing all of the components. Any one of the bands can be recreated - here the SPIRE 250 μm band is reconstructed. The result is directly comparable to the original observations (left). On the right is the ratio between model and observations. It can be seen that in this case, the dust emission has been well accounted for.

4 Results and discussion

4.1 Missing gas

After having inverted the dust emission and reconstructed the modelled emission (e.g. Fig.2), there may be a significant fraction of the dust emission which is not accounted for. This may be due to dust associated with ionised gas, as we do not include components of this gas phase. Another possibility is that the CO being used is no longer tracing all the molecular gas as it has become optically thick, or the CO molecules are freezing out onto the dust grains. An interesting example of this excess residue is shown for the 250 μm band in Fig.3. A central core is left behind after the inversion.

4.2 Hot cores

The temperature of the dust in the clumps with respect to the diffuse component associated with the HI is an interesting point. One might suppose that the dust in the clump should be colder as it will be more shielded from the interstellar radiation field. However, when comparing the dust temperature in the clumps to the dust temperature associated with the HI (displayed in Fig.4), a number of the molecular cores are found to have significantly warmer dust than the HI component. This would seem to suggest an internal source of heating in the clumps, which may indicate that some stage of star formation has begun.

Interestingly, the 'hot' cores are not distributed randomly across the field, but are clustered near l=30.5, b=0.5. In Fig4 the CO clumps have been plotted on top of the dust temperature map of Bernard et al. (2010). The clumps with a higher temperature than the HI are represented by a circle and the rest are represented by squares. Many of the hotter cores are associated with colder spots in the temperature map. This is because the temperature map is a mean temperature of the entire line of sight whereas here we are separating the different line of sight contributions.

There are many candidate MYSO (from the RMSX survey, Mottram et al. 2010), plotted as red stars, surrounding the 'hot' cores. None of these coincide with a hot core so this may be the sign of triggered star formation. Follow up observations of the 'hot' cores will help to reveal their true identity.

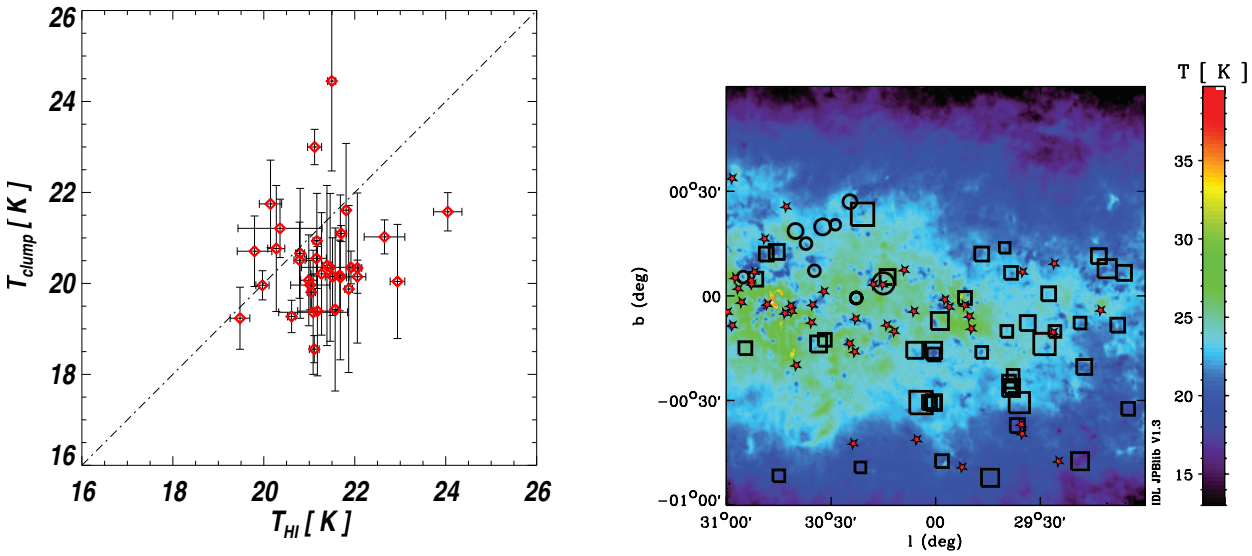

Fig. 4. Left: Dust temperature in the CO clumps vs the dust temperature in the HI gas. A number of the CO clumps show dust which is significantly hotter than the dust in the HI gas. Right: Distribution of the clumps with respect to a dust temperature map of the l=30 SDP field. The clumps with dust hotter than the HI are plotted as circles, the others as squares. Candidate MYSO from the Red MSX survey are plotted as red stars.

5 Conclusions

This new method for dust emission inversion can be applied to the entire Hi-GAL survey, where molecular and atomic observations exist. It will be possible to explore the dust properties in an unprecedented number of cores. Furthermore, this inversion singles out interesting cores for follow up study. A number of candidate hot molecular cores have already been identified as well as cores where the dust emissivity may be enhanced in their cores.

References

Bernard, J., Paradis, D., Marshall, D. J., et al. 2010, A&A, 518, L88
Giard, M., Lamarre, J. M., Pajot, F., & Serra, G. 1994, A&A, 286, 203
Jackson, J. M., Rathborne, J. M., Shah, R. Y., et al. 2006, ApJS, 163, 145
Molinari, S., Swinyard, B., Bally, J., et al. 2010a, A&A, 518, L100
Molinari, S., Swinyard, B., Bally, J., et al. 2010b, PASP, 122, 314
Mottram, J. C., Hoare, M. G., Lumsden, S. L., et al. 2010, A&A, 510, A89
Paladini, R., Montier, L., Giard, M., et al. 2007, A&A, 465, 839
Rathborne, J.M., Johnson, A.M., Jackson, J.M., Shah, R. Y., & Simon, R. 2009,ApJS, 182, 131
Roman-Duval, J., Jackson, J. M., Heyer, M., et al. 2009, ApJ, 699, 1153
Sodroski, T. J., Odegard, N., Arendt, R. G., et al. 1997, ApJ, 480, 173
Stepnik, B., Abergel, A., Bernard, J.-P., et al. 2003, A&A, 398, 551
Stil, J. M., Taylor, A. R., Dickey, J. M., et al. 2006, AJ, 132, 1158